Issued: 4/2009

JUNCAP2
version 200.3

A.J. Scholten, M. Durand, G.D.J. Smit, and D.B.M. Klaassen
(NXP-TSMC Research Center)

Unclassified Report

Authors' address A.J. Scholten; andries.scholten@nxp.com
G.D.J. Smit; gert-jan.smit@nxp.com
D.B.M. Klaassen; d.b.m.klaassen@nxp.com

Title:	JUNCAP2; version 200.3
Author(s):	A.J. Scholten, M. Durand, G.D.J. Smit, and D.B.M. Klaassen (NXP-TSMC Research Center)
Reviewer(s):	
Technical Note:	NXP-R-TN-00000
Additional Numbers:	
Subcategory:	
Project:	Compact modelling
Customer:	NXP Semiconductors

Abstract: This report documents the JUNCAP2 compact model which describes the behavior of the junction diodes in a MOSFET. The JUNCAP2 model describes the following physical effects:

- geometrical scaling: bottom, STI-edge, and gate-edge components;

- depletion capacitance;

- ideal diode current;

- Shockley-Read-Hall generation/recombination current, both in forward and reverse mode of operation;

- trap-assisted tunneling current, both in forward and reverse mode of operation;

- band-to-band tunneling current;

- avalanche and breakdown;

- shot noise.

History of model and documentation

Introduction

The first version of the compact MOS model JUNCAP2, Level 200, has been released to the public domain in April 2005. Changes and additions to the model are documented by adapting or extending the documentation in this Report.

History of the model

April 2005 Release of JUNCAP2, level 200 as part of SiMKit 2.1. A Verilog-A implementation is made available as well.

August 2005 Release of JUNCAP2, level 200.1 as part of SiMKit 2.2. Similar to the previous version, a Verilog-A implementation of the JUNCAP2-model is made available as well. Focus of this release was mainly on the optimization of the evaluation speed of JUNCAP2. This new version is fully parameter compatible with the previous version.

The following changes have been made:

- limiting of charge model and of $w_{\mathrm{SRH,step}}$ is now based on the minimum of three built-in voltages, instead of separate limiting for bottom, STI-edge, and gate-edge component;

- limiting of V_{j} to $V_{\mathrm{j,SRH}}$ in Shockley-Read-Hall model replaced by adopting VMAX/IMAX-construction of ideal-current model; subsequently the original $V_{\mathrm{j,SRH2}}$ has been renamed into $V_{\mathrm{j,SRH}}$;

- limiting of V_{AK} to V_{j} in charge model changed from ln-exp type into so-called hyp5 function; limiting of V_{AK} to $V_{\mathrm{j,SRH}}$ (i.e. the previous $V_{\mathrm{j,SRH2}}$) in Shockley-Read-Hall model changed from ln-exp type into so-called hyp2 function.

- expression for Δw_{SRH} rewritten im more concise form (mathematically identical to previous version), see Eq. (4.43).

August 2006 Release of JUNCAP2, level 200.2. In this version a problem that was found in the band-to-band tunneling model is solved.

October 2007 Release of JUNCAP2, level 200.3 as part of SiMKit 3.0. In this version, JUNCAP Express is introduced. The Express model can be invoked by setting the parameter **SWJUNEXP** to 1. This results in a very significant decrease (about a factor 5 in typical situations) of the JUNCAP2 model evaluation time. Yet the Express model was created to give only very limited loss of accuracy under typical operating conditions of the device.

November 2008 Release of JUNCAP2, level 200.3.3 as part of SiMKit 3.2. In this version, a bug w.r.t. the JUNCAP Express parameter **FJUNQ** has been corrected.

History of the documentation

April 2005 First release of JUNCAP2, level 200 documentation.

August 2005 Documentation updated for JUNCAP2, level 200.1 release. Section A has been added to document the so-called hyp-functions introduced in level 200.1.

March 2006 Documentation update. Section 6.7 has been added.

June 2006   Documentation update. Error in Eq. (4.51), which defines b_{TAT}, is corrected.

August 2006   Documentation updated with modified band-to-band tunneling equations: Eqs. (4.62) and (4.63) added, Eqs. (4.64) and (4.65) modified, and constant ΔV_{bi} added to list of model constants in Section 3.2. Additional information on simulation times associated to the various physical effects in the model added to Section 6.7.

October 2007   Documentation updated for JUNCAP2 version 200.3, including JUNCAP2 Express. Look and feel of documentation brought in closer agreement with PSP documentation.

April 2009   Documentation updated for JUNCAP2 version 200.3.3. Eqs. (4.108), (4.109), and (4.110) are brought in accordance with **FJUNQ**-related bugfix made in 200.3.3 (released in November 2008). In addition, some typos have been corrected.

Contents

Section 1

Introduction

The JUNCAP2 model is intended to describe the behavior of the diodes that are formed by the source, drain, or well-to-bulk junctions in MOSFETs. It is the successor of the JUNCAP level=1 model [1].

Whereas the JUNCAP level=1 model gives a satisfactory description of the junction capacitances, its description of diode leakage currents is rather poor for present-day CMOS technologies. This is due to ever increasing doping concentrations in the junctions, leading to increasing electric fields. Due to these high electric fields, leakage mechanisms such as trap-assisted tunneling and band-to-band tunneling have gained importance to such an extent, that they are starting to contribute to the MOSFET off-state current. Thus, accurate modelling of these leakage currents is called for.

In addition to its relevance for advanced CMOS technologies, accurate junction modelling is also relevant for partially depleted SOI (PDSOI). Here, a small positive voltage at the floating body exists, which is determined by the equilibrium between impact ionization and gate current on one hand and current through the source junction on the other hand. Due to the back-gate effect, this small positive floating body voltage gives rise to additional drain current, where it is visible as the so-called "kink effect". Thus, for PDSOI applications, accurate junction modelling in the low-forward regime is required.

Section 2

Summary of physics behind JUNCAP2

The JUNCAP2 model has been developed for the description of source and drain junctions in MOSFETs. The model equations have been developed for symmetrical junctions of arbitrary grading coefficient. The following physical effects have been included:

Geometrical scaling

JUNCAP2 models the capacitances and currents of bottom-, STI-edge, and gate-edge components. This is illustrated in Figs. 2.1 and 2.2.

Depletion capacitance

The depletion capacitance model, similar to JUNCAP1, is a standard textbook equation. It has been safeguarded against numerical overflow in the forward mode of operation.

Ideal current

The ideal diode current is modeled using the ideal-case Shockley equation. The bandgap has been made a free parameter to be able to tune the temperature dependence. No (unphysical) ideality factor has been included. Non-idealities are modeled with physics-based equations, as outlined below.

Shockley-Read-Hall current

The Shockley-Read-Hall current is calculated by integrating the Shockley-Read-Hall generation-recombination rate over the depletion region. This is done for arbitrary grading coefficient and results in a single-piece expression in forward and reverse mode of operation.

Trap-assisted tunneling current

The trap-assisted tunneling current is calculated in a similar fashion as the Shockley-Read-Hall current. Now also the field-enhancement factor [2] is taken into account in the calculation. In contrast to e.g. Diode Level 500 [1], the calculation is not based on the low-field approximation of this field-enhancement factor, but is generally valid for both low and high fields. The calculation results in a single-piece expression which is valid in both the forward and reverse regime, and for arbitrary grading coefficient.

Band-to-band tunneling current

For the band-to-band tunneling current, a physical model similar to the Diode Level 500 [1] equation has been implemented. Some additional freedom in fitting the (small) temperature dependence of this current is provided.

Avalanche breakdown

For avalanche breakdown, an expression has been derived which is a simplified form of the Diode Level 500 [1] equations for this phenomenon. In comparison with Diode Level 500, some additional freedom in fitting the onset to breakdown is provided.

Noise

In partially depleted silicon-on-insulator (PD SOI), the shot noise of the junction current is important because, together with the shot noise of the impact ionization current of the MOSFET, it leads to additional Lorentzian noise in the drain current [3]. Therefore, shot noise has been implemented in JUNCAP2.
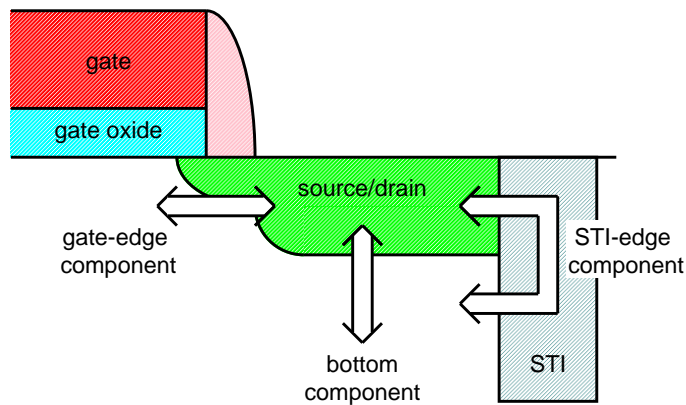

Figure 2.1: The three contributions to the source/drain junction of a MOSFET
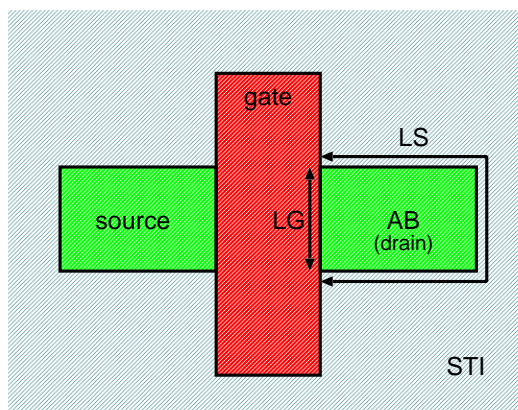
Figure 2.2: Schematic top view of the MOSFET. The meaning of the instance parameters **AB**, **LS**, and **LG** is indicated in the drain region.

Section 3

Model parameters and constants

3.1 Physical Constants

No.	Symbol	Unit	Value	Description
1	T_0	K	273.15	offset between Celsius and Kelvin temperature scale
2	k_{B}	J/K	$1.3806505 \cdot 10^{-23}$	Boltzmann constant
3	q	C	$1.6021918 \cdot 10^{-19}$	elementary charge
4	$\hbar$	$\mathrm{J} \cdot \mathrm{s}$	$1.05457168 \cdot 10^{-34}$	reduced Planck constant
5	m_0	kg	$9.1093826 \cdot 10^{-31}$	electron rest mass
6	ϵ_0	F/m	$8.85418782 \cdot 10^{-12}$	Permittivity of vacuum
7	$\epsilon_{\mathrm{r,Si}}$	–	11.8	Relative permittivity of silicon

3.2 Other constants

No.	Symbol	Unit	Value	Description
1	$T_{\min}$	°C	-250	minimum temperature for model equations
2	$V_{\mathrm{bi,low}}$	V	0.050	lower boundary for built-in voltage
3	a	–	2	sets upper limit of forward capacitance to $a \cdot C_{\mathrm{jo}}$
4	ϵ_{ch}	–	0.1	smoothing constant for charge model
5	ΔV_{bi}	–	0.050	voltage difference used in band-to-band tunneling model
6	ϵ_{av}	–	10^{-6}	smoothing constant for effective voltage in avalanche model
7	$V_{\mathrm{br,max}}$	V	10^3	upper limit for **VBR**; for larger values, avalanche model is switched off
8	α_{av}	–	0.999	below $-\alpha_{\mathrm{av}} \cdot$ **VBR** avalanche model is linearized
9	$V_{\mathrm{max,large}}$	V	10^8	value assigned to $V_{\max}$ when I_{DSAT} is zero.
10	a_{erfc}	–	0.29214664	parameter in erfc approximation
11	p_{erfc}	–	$\sqrt{\pi} \cdot a_{\mathrm{erfc}}$	parameter in erfc approximation

. . . continued from previous page

No.	Symbol	Unit	Value	Description
12	b_{erfc}	–	$\frac{6-5\cdot a_{\text{erfc}}-p_{\text{erfc}}^{-2}}{3}$	parameter in erfc approximation
13	c_{erfc}	–	$1 - a_{\text{erfc}} - b_{\text{erfc}}$	parameter in erfc approximation

3.3 Instance parameters

No.	Name	Unit	Default	Min.	Max.	Description
0	**AB**	m^2	10^{-12}	0	–	junction area
1	**LS**	m	10^{-6}	0	–	STI-edge part of junction perimeter
2	**LG**	m	10^{-6}	0	–	gate-edge part of junction perimeter
3	**MULT**	–	1	0	–	multiplication factor

3.4 Model parameters

No.	Name	Unit	Default	Min.	Max.	Description
0	**LEVEL**	–	200	200	200	model selection parameter
1	**TYPE**	–	1	–	–	switch (-1 or 1) to select $p-n$ and $n-p$ junction
2	**TRJ**	°C	21	T_{min}	–	reference temperature
3	**SWJUNEXP**	–	0	0	1	flag for JUNCAP Express; $0 \leftrightarrow$ full JUNCAP2 model, $1 \leftrightarrow$ Express model
4	**DTA**	°C	0	–	–	temperature offset with respect to ambient temperature
5	**IMAX**	A	1000	1×10^{-12}	–	maximum current up to which forward current behaves exponentially
			Capacitance parameters			
6	**CJORBOT**	F/m^2	10^{-3}	10^{-12}	–	zero-bias capacitance per unit-of-area of bottom component
7	**CJORSTI**	F/m	10^{-9}	10^{-18}	–	zero-bias capacitance per unit-of-length of STI-edge component
8	**CJORGAT**	F/m	10^{-9}	10^{-18}	–	zero-bias capacitance per unit-of-length of gate-edge component
9	**VBIRBOT**	V	1	$V_{\text{bi,low}}$	–	built-in voltage at the reference temperature of bottom component
10	**VBIRSTI**	V	1	$V_{\text{bi,low}}$	–	built-in voltage at the reference temperature of STI-edge component
11	**VBIRGAT**	V	1	$V_{\text{bi,low}}$	–	built-in voltage at the reference temperature of gate-edge component
12	**PBOT**	–	0.5	0.05	0.95	grading coefficient of bottom component
13	**PSTI**	–	0.5	0.05	0.95	grading coefficient of STI-edge component

. . . continued from previous page

No.	Name	Unit	Default	Min.	Max.	Description
14	**PGAT**	–	0.5	0.05	0.95	grading coefficient of gate-edge component
Ideal-current parameters						
15	**PHIGBOT**	V	1.16	–	–	zero-temperature bandgap voltage of bottom component
16	**PHIGSTI**	V	1.16	–	–	zero-temperature bandgap voltage of STI-edge component
17	**PHIGGAT**	V	1.16	–	–	zero-temperature bandgap voltage of gate-edge component
18	**IDSATRBOT**	A/m^2	10^{-12}	0	–	saturation current density at the reference temperature of bottom component
19	**IDSATRSTI**	A/m	10^{-18}	0	–	saturation current density at the reference temperature of STI-edge component
20	**IDSATRGAT**	A/m	10^{-18}	0	–	saturation current density at the reference temperature of gate-edge component
Shockley-Read-Hall parameters						
21	**CSRHBOT**	A/m^3	10^2	0	–	Shockley-Read-Hall prefactor of bottom component
22	**CSRHSTI**	A/m^2	10^{-4}	0	–	Shockley-Read-Hall prefactor of STI-edge component
23	**CSRHGAT**	A/m^2	10^{-4}	0	–	Shockley-Read-Hall prefactor of gate-edge component
24	**XJUNSTI**	m	10^{-7}	10^{-9}	–	junction depth of STI-edge component
25	**XJUNGAT**	m	10^{-7}	10^{-9}	–	junction depth of gate-edge component
Trap-assisted tunneling parameters						
26	**CTATBOT**	A/m^3	10^2	0	–	trap-assisted tunneling prefactor of bottom component
27	**CTATSTI**	A/m^2	10^{-4}	0	–	trap-assisted tunneling prefactor of STI-edge component
28	**CTATGAT**	A/m^2	10^{-4}	0	–	trap-assisted tunneling prefactor of gate-edge component
29	**MEFFTATBOT**	–	0.25	0.01	–	relative effective mass for trap-assisted tunneling of bottom component
30	**MEFFTATSTI**	–	0.25	0.01	–	relative effective mass for trap-assisted tunneling of STI-edge component
31	**MEFFTATGAT**	–	0.25	0.01	–	relative effective mass for trap-assisted tunneling of gate-edge component
Band-to-band tunneling parameters						
32	**CBBTBOT**	AV^{-3}	10^{-12}	0	–	band-to-band tunneling prefactor of bottom component
33	**CBBTSTI**	AV^{-3}m	10^{-18}	0	–	band-to-band tunneling prefactor of STI-edge component
34	**CBBTGAT**	AV^{-3}m	10^{-18}	0	–	band-to-band tunneling prefactor of gate-edge component

continued on next page. . .

. . . continued from previous page

No.	Name	Unit	Default	Min.	Max.	Description
35	**FBBTRBOT**	Vm^{-1}	10^9	−	−	normalization field at the reference temperature for band-to-band tunneling of bottom component
36	**FBBTRSTI**	Vm^{-1}	10^9	−	−	normalization field at the reference temperature for band-to-band tunneling of STI-edge component
37	**FBBTRGAT**	Vm^{-1}	10^9	−	−	normalization field at the reference temperature for band-to-band tunneling of gate-edge component
38	**STFBBTBOT**	K^{-1}	-10^{-3}	−	−	temperature scaling parameter for band-to-band tunneling of bottom component
39	**STFBBTSTI**	K^{-1}	-10^{-3}	−	−	temperature scaling parameter for band-to-band tunneling of STI-edge component
40	**STFBBTGAT**	K^{-1}	-10^{-3}	−	−	temperature scaling parameter for band-to-band tunneling of gate-edge component
Avalanche and breakdown parameters						
41	**VBRBOT**	V	10	0.1	−	breakdown voltage of bottom component
42	**VBRSTI**	V	10	0.1	−	breakdown voltage of STI-edge component
43	**VBRGAT**	V	10	0.1	−	breakdown voltage of gate-edge component
44	**PBRBOT**	V	4	0.1	−	breakdown onset tuning parameter of bottom component
45	**PBRSTI**	V	4	0.1	−	breakdown onset tuning parameter of STI-edge component
46	**PBRGAT**	V	4	0.1	−	breakdown onset tuning parameter of gate-edge component
JUNCAP Express Parameters						
47	**VJUNREF**	V	2.5	0.5	−	typical maximum junction voltage; usually about $2 \cdot V_{\text{sup}}$
48	**FJUNQ**	V	0.03	0	−	fraction below which junction capacitance components are neglected

Section 4

Model equations

4.1   Internal parameters

In this section, bias-independent internal parameters are calculated. All computations in this section are dependent on model/instance parameters and temperature only; they are independent of bias. Therefore, these equations need to be evaluated in the initialization phase only.

Thermal voltage

$$T_{\text{KR}} = T_0 + \textbf{TRJ} \tag{4.1}$$

$$T_{\text{KD}} = T_0 + \max(T_{\text{A}} + \textbf{DTA}, T_{\min}) \tag{4.2}$$

$$\phi_{\text{TR}} = \frac{k_{\text{B}} \cdot T_{\text{KR}}}{q} \tag{4.3}$$

$$\phi_{\text{TD}} = \frac{k_{\text{B}} \cdot T_{\text{KD}}}{q} \tag{4.4}$$

Band gap

$$\Delta\phi_{\text{GR}} = -\frac{7.02 \cdot 10^{-4} \cdot T_{\text{KR}}^2}{1108.0 + T_{\text{KR}}} \tag{4.5}$$

$$\phi_{\text{GR,bot}} = \textbf{PHIGBOT} + \Delta\phi_{\text{GR}} \tag{4.6}$$

$$\phi_{\text{GR,sti}} = \textbf{PHIGSTI} + \Delta\phi_{\text{GR}} \tag{4.7}$$

$$\phi_{\text{GR,gat}} = \textbf{PHIGGAT} + \Delta\phi_{\text{GR}} \tag{4.8}$$

$$\Delta\phi_{\text{GD}} = -\frac{7.02 \cdot 10^{-4} \cdot T_{\text{KD}}^2}{1108.0 + T_{\text{KD}}} \tag{4.9}$$

$$\phi_{\text{GD,bot}} = \textbf{PHIGBOT} + \Delta\phi_{\text{GD}} \tag{4.10}$$

$$\phi_{\text{GD,sti}} = \textbf{PHIGSTI} + \Delta\phi_{\text{GD}} \tag{4.11}$$

$$\phi_{\text{GD,gat}} = \textbf{PHIGGAT} + \Delta\phi_{\text{GD}} \tag{4.12}$$

Intrinsic carrier concentration

$$F_{\text{TD,bot}} = \left(\frac{T_{\text{KD}}}{T_{\text{KR}}}\right)^{1.5} \cdot \exp\left(\frac{\phi_{\text{GR,bot}}}{2 \cdot \phi_{\text{TR}}} - \frac{\phi_{\text{GD,bot}}}{2 \cdot \phi_{\text{TD}}}\right) \tag{4.13}$$

$$F_{\text{TD,sti}} = \left(\frac{T_{\text{KD}}}{T_{\text{KR}}}\right)^{1.5} \cdot \exp\left(\frac{\phi_{\text{GR,sti}}}{2 \cdot \phi_{\text{TR}}} - \frac{\phi_{\text{GD,sti}}}{2 \cdot \phi_{\text{TD}}}\right) \tag{4.14}$$

$$F_{\text{TD,gat}} = \left(\frac{T_{\text{KD}}}{T_{\text{KR}}}\right)^{1.5} \cdot \exp\left(\frac{\phi_{\text{GR,gat}}}{2 \cdot \phi_{\text{TR}}} - \frac{\phi_{\text{GD,gat}}}{2 \cdot \phi_{\text{TD}}}\right) \tag{4.15}$$

Saturation current density at device temperature

$$I_{\text{DSAT,bot}} = \textbf{IDSATRBOT} \cdot F_{\text{TD,bot}}{}^2 \tag{4.16}$$

$$I_{\text{DSAT,sti}} = \textbf{IDSATRSTI} \cdot F_{\text{TD,sti}}{}^2 \tag{4.17}$$

$$I_{\text{DSAT,gat}} = \textbf{IDSATRGAT} \cdot F_{\text{TD,gat}}{}^2 \tag{4.18}$$

Determination of V_{max}

$$V_{\text{max,bot}} = \begin{cases} V_{\text{max,large}} & \text{if } I_{\text{DSAT,bot}} \cdot \textbf{AB} = 0 \\[2ex] \phi_{\text{TD}} \cdot \ln\left(\dfrac{\textbf{IMAX}}{I_{\text{DSAT,bot}} \cdot \textbf{AB}} + 1\right) & \text{if } I_{\text{DSAT,bot}} \cdot \textbf{AB} \neq 0 \end{cases} \tag{4.19}$$

$$V_{\text{max,sti}} = \begin{cases} V_{\text{max,large}} & \text{if } I_{\text{DSAT,sti}} \cdot \textbf{LS} = 0 \\[2ex] \phi_{\text{TD}} \cdot \ln\left(\dfrac{\textbf{IMAX}}{I_{\text{DSAT,sti}} \cdot \textbf{LS}} + 1\right) & \text{if } I_{\text{DSAT,sti}} \cdot \textbf{LS} \neq 0 \end{cases} \tag{4.20}$$

$$V_{\text{max,gat}} = \begin{cases} V_{\text{max,large}} & \text{if } I_{\text{DSAT,gat}} \cdot \textbf{LG} = 0 \\[2ex] \phi_{\text{TD}} \cdot \ln\left(\dfrac{\textbf{IMAX}}{I_{\text{DSAT,gat}} \cdot \textbf{LG}} + 1\right) & \text{if } I_{\text{DSAT,gat}} \cdot \textbf{LG} \neq 0 \end{cases} \tag{4.21}$$

$$V_{\text{max}} = \min\left(V_{\text{max,bot}}, V_{\text{max,sti}}, V_{\text{max,gat}}\right) \tag{4.22}$$

Built-in voltages

$$U_{\text{bi,bot}} = \textbf{VBIRBOT} \cdot \frac{T_{\text{KD}}}{T_{\text{KR}}} - 2 \cdot \phi_{\text{TD}} \cdot \ln F_{\text{TD,bot}} \tag{4.23}$$

$$V_{\text{bi,bot}} = U_{\text{bi,bot}} + \phi_{\text{TD}} \cdot \ln\left[1 + \exp\left(\frac{V_{\text{bi,low}} - U_{\text{bi,bot}}}{\phi_{\text{TD}}}\right)\right] \tag{4.24}$$

$$U_{\text{bi,sti}} = \textbf{VBIRSTI} \cdot \frac{T_{\text{KD}}}{T_{\text{KR}}} - 2 \cdot \phi_{\text{TD}} \cdot \ln F_{\text{TD,sti}} \tag{4.25}$$

$$V_{\text{bi,sti}} = U_{\text{bi,sti}} + \phi_{\text{TD}} \cdot \ln\left[1 + \exp\left(\frac{V_{\text{bi,low}} - U_{\text{bi,sti}}}{\phi_{\text{TD}}}\right)\right] \tag{4.26}$$

$$U_{\mathrm{bi,gat}} = \mathbf{VBIRGAT} \cdot \frac{T_{\mathrm{KD}}}{T_{\mathrm{KR}}} - 2 \cdot \phi_{\mathrm{TD}} \cdot \ln F_{\mathrm{TD,gat}} \tag{4.27}$$

$$V_{\mathrm{bi,gat}} = U_{\mathrm{bi,gat}} + \phi_{\mathrm{TD}} \cdot \ln \left[1 + \exp \left(\frac{V_{\mathrm{bi,low}} - U_{\mathrm{bi,gat}}}{\phi_{\mathrm{TD}}} \right) \right] \tag{4.28}$$

Determination of $V_{\mathrm{F,min}}$ and V_{ch}

$$V_{\mathrm{bi,min}} = \min \left(V_{\mathrm{bi,bot}}, V_{\mathrm{bi,sti}}, V_{\mathrm{bi,gat}} \right) \tag{4.29}$$

Note: in taking this minimum, only the V_{bi} of the relevant contributions are taken into account. For example, when **AB** $= 0$, $V_{\mathrm{bi,bot}}$ is not taken into account.

$$V_{\mathrm{F,min}} = \begin{cases} V_{\mathrm{bi,min}} \cdot \left(1 - a^{-1/\mathbf{PBOT}} \right) & \text{if } V_{\mathrm{bi,min}} = V_{\mathrm{bi,bot}} \\ V_{\mathrm{bi,min}} \cdot \left(1 - a^{-1/\mathbf{PSTI}} \right) & \text{if } V_{\mathrm{bi,min}} = V_{\mathrm{bi,sti}} \\ V_{\mathrm{bi,min}} \cdot \left(1 - a^{-1/\mathbf{PGAT}} \right) & \text{if } V_{\mathrm{bi,min}} = V_{\mathrm{bi,gat}} \end{cases} \tag{4.30}$$

$$V_{\mathrm{ch}} = \epsilon_{\mathrm{ch}} \cdot V_{\mathrm{bi,min}} \tag{4.31}$$

4.2 The juncap-function

This section describes a function which contains the full (electrical) characteristics of the JUNCAP2 model. In the actual model it will be evaluated up to three times: for the bottom, STI-edge, and gate-edge components of the model. The definition of the hyp-functions are given in Section A.

Input parameters of the juncap-function

No.	Name	Description
0	V_{AK}	in case **TYPE** $= 1$: voltage between anode (p-side) and cathode (n-side); in case **TYPE** $= -1$: voltage between cathode and anode
1	T_{KR}	reference temperature in Kelvin
2	T_{KD}	device temperature in Kelvin
3	ϕ_{TD}	thermal voltage at device temperature
4	ϕ_{GD}	bandgap voltage at device temperature
5	F_{TD}	intrinsic carrier concentration at device temperature, divided by that at reference temperature
6	I_{DSAT}	saturation current density of ideal current
7	V_{bi}	built-in voltage at the device temperature
8	$V_{\mathrm{bi,min}}$	minimum V_{bi} of bottom, STI-edge, and gate-edge contribution
9	$V_{\mathrm{F,min}}$	limiting voltage for charge model
10	V_{ch}	smoothing constant for transition $V_{\mathrm{F,min}} \to V_{\mathrm{ch}}$ in charge model
11	**VMAX**	maximum voltage up to which forward current behaves exponentially
12	**CJOR**	zero-bias capacitance per unit-of-area
13	**VBIR**	built-in voltage at the reference temperature

. . . continued from previous page

No.	Name	Description
14	**P**	grading coefficient
15	**CSRH**	Shockley-Read-Hall prefactor
16	**XJUN**	junction depth
17	**CTAT**	trap-assisted tunneling prefactor
18	**MEFFTAT**	effective mass (in units of m_0) for trap-assisted tunneling
19	**CBBT**	band-to-band tunneling prefactor
20	**FBBTR**	normalization field at the reference temperature for band-to-band tunneling
21	**STFBBT**	temperature scaling parameter for band-to-band tunneling
22	**VBR**	breakdown voltage
23	**PBR**	breakdown onset tuning parameter

Outputs of the juncap-function

No.	Name	Description
0	$I'_{\rm j}$	junction current per unit of area or length
1	$Q'_{\rm j}$	junction charge per unit of area or length

Definition of the juncap-function

Junction charge

$$C_{\rm jo} = \textbf{CJOR} \cdot \left(\frac{\textbf{VBIR}}{V_{\rm bi}} \right)^{\textbf{P}} \tag{4.32}$$

$$V_{\rm j} = {\rm hyp}_5(V_{\rm AK}; V_{\rm F,min}, V_{\rm ch}) \tag{4.33}$$

$$Q'_{\rm j} = \left\{ \frac{C_{\rm jo} \cdot V_{\rm bi}}{1 - \textbf{P}} \cdot \left[1 - \left(1 - \frac{V_{\rm j}}{V_{\rm bi}} \right)^{1-\textbf{P}} \right] + a \cdot C_{\rm jo} \cdot (V_{\rm AK} - V_{\rm j}) \right\} \tag{4.34}$$

Ideal current

$$M_{\rm ID} = \begin{cases} \exp \left(\dfrac{V_{\rm AK}}{\phi_{\rm TD}} \right) & \text{if } V_{\rm AK} < V_{\rm max} \\[3mm] \left(1 + \dfrac{V_{\rm AK} - \textbf{VMAX}}{\phi_{\rm TD}} \right) \cdot \exp \left(\dfrac{\textbf{VMAX}}{\phi_{\rm TD}} \right) & \text{if } V_{\rm AK} \geq V_{\rm max} \end{cases} \tag{4.35}$$

$$I'_{\rm D} = (M_{\rm ID} - 1) \cdot I_{\rm DSAT} \tag{4.36}$$

Shockley-Read-Hall current

Note: if **CSRH** = **CTAT** = 0, Eqs. (4.37). . . (4.46) should be skipped and $I'_{\rm SRH} = 0$.

$$z_{\rm inv} = \sqrt{M_{\rm ID}} \tag{4.37}$$

$$z = \frac{1}{z_{\text{inv}}} \tag{4.38}$$

$$\psi^* = \begin{cases} \phi_{\text{TD}} \cdot \ln\left[z + 2 + \sqrt{(z+1) \cdot (z+3)}\right] & \text{if } V_{\text{AK}} > 0 \\[2mm] \dfrac{-V_{\text{AK}}}{2} + \phi_{\text{TD}} \cdot \ln\left[1 + 2 \cdot z_{\text{inv}} + \sqrt{(1 + z_{\text{inv}}) \cdot (1 + 3 \cdot z_{\text{inv}})}\right] & \text{if } V_{\text{AK}} \leq 0 \end{cases} \tag{4.39}$$

$$V_{\text{j,lim}} = V_{\text{bi,min}} - 2 \cdot \psi^* \tag{4.40}$$

$$V_{\text{j,SRH}} = \text{hyp}_2(V_{\text{AK}}; V_{\text{j,lim}}, \phi_{\text{TD}}) \tag{4.41}$$

$$w_{\text{SRH,step}} = 1 - \sqrt{1 - \frac{2 \cdot \psi^*}{V_{\text{bi}} - V_{\text{j,SRH}}}} \tag{4.42}$$

$$\Delta w_{\text{SRH}} = \left(\frac{w_{\text{SRH,step}}^2 \cdot \ln w_{\text{SRH,step}}}{1 - w_{\text{SRH,step}}} + w_{\text{SRH,step}}\right) \cdot (1 - 2 \cdot \mathbf{P}) \tag{4.43}$$

$$w_{\text{SRH}} = w_{\text{SRH,step}} + \Delta w_{\text{SRH}} \tag{4.44}$$

$$W_{\text{dep}} = \frac{\mathbf{XJUN} \cdot \epsilon_{\text{Si}}}{\mathbf{CJOR}} \cdot \left(\frac{V_{\text{bi}} - V_{\text{j,SRH}}}{\mathbf{VBIR}}\right)^{\mathbf{P}} \tag{4.45}$$

$$I'_{\text{SRH}} = \mathbf{CSRH} \cdot F_{\text{TD}} \cdot (z_{\text{inv}} - 1) \cdot w_{\text{SRH}} \cdot W_{\text{dep}} \tag{4.46}$$

Trap-assisted-tunneling current

Note: if **CTAT** = 0, Eqs. (4.47)... (4.61) should be skipped and $I'_{\text{TAT}} = 0$.

$$F_{\text{max}} = \frac{V_{\text{bi}} - V_{\text{j,SRH}}}{W_{\text{dep}} \cdot (1 - \mathbf{P})} \tag{4.47}$$

$$m_{\text{eff}} = \mathbf{MEFFTAT} \cdot m_0 \tag{4.48}$$

$$\Delta E = \max\left(\frac{\phi_{\text{GD}}}{2}, \phi_{\text{TD}}\right) \tag{4.49}$$

$$a_{\text{TAT}} = \frac{\Delta E}{\phi_{\text{TD}}} \tag{4.50}$$

$$b_{\text{TAT}} = \frac{\sqrt{32 \cdot m_{\text{eff}} \cdot q \cdot \Delta E^3}}{3 \cdot \hbar \cdot F_{\text{max}}} \tag{4.51}$$

$$u'_{\text{max}} = \left(\frac{2 \cdot a_{\text{TAT}}}{3 \cdot b_{\text{TAT}}}\right)^2 \tag{4.52}$$

$$u_{\text{max}} = \sqrt{\frac{u'_{\text{max}}{}^2}{u'_{\text{max}}{}^2 + 1}} \tag{4.53}$$

$$w_{\Gamma} = \left(1 + b_{\text{TAT}} \cdot u_{\text{max}}{}^{3/2}\right)^{\frac{\mathbf{P}}{\mathbf{P}-1}} \tag{4.54}$$

$$w_{\text{TAT}} = \frac{w_{\text{SRH}} \cdot w_{\Gamma}}{w_{\text{SRH}} + w_{\Gamma}} \tag{4.55}$$

$$k_{\text{TAT}} = \sqrt{\frac{3 \cdot b_{\text{TAT}}}{8 \cdot \sqrt{u_{\max}}}} \tag{4.56}$$

$$l_{\text{TAT}} = \frac{4 \cdot a_{\text{TAT}}}{3 \cdot b_{\text{TAT}}} \cdot \sqrt{u_{\max}} - u_{\max} \tag{4.57}$$

$$m_{\text{TAT}} = \frac{2 \cdot a_{\text{TAT}}^2}{3 \cdot b_{\text{TAT}}} \cdot \sqrt{u_{\max}} - a_{\text{TAT}} \cdot u_{\max} + \frac{b_{\text{TAT}}}{2} \cdot u_{\max}^{3/2} \tag{4.58}$$

$$\text{erfcapprox}(y) = \begin{cases} t_{\text{erfc}} = \begin{cases} \dfrac{1}{1 + p_{\text{erfc}} \cdot y} & \text{if } y > 0 \\[2mm] \dfrac{1}{1 - p_{\text{erfc}} \cdot y} & \text{if } y \leq 0 \end{cases} \\[6mm] \text{erfcapprox}^+ = \left(a_{\text{erfc}} \cdot t_{\text{erfc}} + b_{\text{erfc}} \cdot t_{\text{erfc}}^2 + c_{\text{erfc}} \cdot t_{\text{erfc}}^3 \right) \cdot \exp(-y^2) \\[4mm] \text{erfcapprox}(y) = \begin{cases} \text{erfcapprox}^+ & \text{if } \quad y > 0 \\[2mm] 2 - \text{erfcapprox}^+ & \text{if } \quad y \leq 0 \end{cases} \end{cases}$$

$$\tag{4.59}$$

$$\Gamma_{\max} = \frac{a_{\text{TAT}} \cdot \exp\left(m_{\text{TAT}}\right) \cdot \text{erfcapprox}\left[k_{\text{TAT}} \cdot (l_{\text{TAT}} - 1)\right] \cdot \sqrt{\pi}}{2 \cdot k_{\text{TAT}}} \tag{4.60}$$

$$I'_{\text{TAT}} = \mathbf{CTAT} \cdot F_{\text{TD}} \cdot (z_{\text{inv}} - 1) \cdot \Gamma_{\max} \cdot w_{\text{TAT}} \cdot W_{\text{dep}} \tag{4.61}$$

Band-to-band tunneling current

Note: if **CBBT** $= 0$, Eqs. (4.64)… (4.67) should be skipped and $I'_{\text{BBT}} = 0$.

$$V_{\text{BBT,lim}} = \min(\mathbf{VBIRBOT}, \mathbf{VBIRSTI}, \mathbf{VBIRGAT}) - \Delta V_{\text{bi}} \tag{4.62}$$

$$V_{\text{BBT}} = \text{hyp}_2(V_{\text{AK}}, V_{\text{BBT,lim}}, \phi_{\text{TR}}) \tag{4.63}$$

$$W_{\text{dep,r}} = \frac{\mathbf{XJUN} \cdot \epsilon_{\text{Si}}}{\mathbf{CJOR}} \cdot \left(\frac{\mathbf{VBIR} - V_{\text{BBT}}}{\mathbf{VBIR}} \right)^{\mathbf{P}} \tag{4.64}$$

$$F_{\text{max,r}} = \frac{\mathbf{VBIR} - V_{\text{BBT}}}{W_{\text{dep,r}} \cdot (1 - \mathbf{P})} \tag{4.65}$$

$$F_{\text{BBT}} = \mathbf{FBBTR} \cdot [1 + \mathbf{STFBBT} \cdot (T_{\text{KD}} - T_{\text{KR}})] \tag{4.66}$$

$$I'_{\text{BBT}} = \mathbf{CBBT} \cdot V_{\text{AK}} \cdot F_{\text{max,r}}^2 \cdot \exp\left(-\frac{F_{\text{BBT}}}{F_{\text{max,r}}} \right) \tag{4.67}$$

Avalanche and breakdown

Note: if **VBR** $> V_{\text{br,max}}$, Eqs. (4.68)... (4.71) should be skipped and $f_{\text{breakdown}} = 1$.

$$V_{\text{av}} = \text{hyp}_2(V_{\text{AK}}; 0, \epsilon_{\text{av}}) \tag{4.68}$$

$$f_{\text{stop}} = \frac{1}{1 - \alpha_{\text{av}}{}^{\textbf{PBR}}} \tag{4.69}$$

$$s_{\text{f}} = -f_{\text{stop}}{}^2 \cdot \alpha_{\text{av}}{}^{\textbf{PBR}-1} \cdot \frac{\textbf{PBR}}{\textbf{VBR}} \tag{4.70}$$

$$f_{\text{breakdown}} = \begin{cases} \dfrac{1}{1 - \left|\dfrac{-V_{\text{av}}}{\textbf{VBR}}\right|^{\textbf{PBR}}} & \text{if } V_{\text{av}} > -\alpha_{\text{av}} \cdot \textbf{VBR} \\[4ex] f_{\text{stop}} + (V_{\text{av}} + \alpha_{\text{av}} \cdot \textbf{VBR}) \cdot s_{\text{f}} & \text{if } V_{\text{av}} \le -\alpha_{\text{av}} \cdot \textbf{VBR} \end{cases} \tag{4.71}$$

Total current

$$I'_{\text{j}} = (I'_{\text{D}} + I'_{\text{SRH}} + I'_{\text{TAT}} + I'_{\text{BBT}}) \cdot f_{\text{breakdown}} \tag{4.72}$$

4.3 The juncap model

The section describes how the full junction characteristics are evaluated by calling the 'juncap function' for each component. If the full JUNCAP2 model is used (that is, when **SWJUNEXP** $= 0$), this calculation is done at each bias point. If the JUNCAP Express option is used (that is, when **SWJUNEXP** $= 1$), this calculation is done during the initialization phase for a small number of bias points only (see Section 4.4).

$$V_{\text{AK}} = \textbf{TYPE} \cdot (V_{\text{A}} - V_{\text{K}}) \tag{4.73}$$

4.3.1 Junction charge

$$\begin{aligned} Q'_{\text{j,bot}} \;=\; & Q'_{\text{j}}(V_{\text{AK}} = V_{\text{AK}}, \; T_{\text{KR}} = T_{\text{KR}}, \; T_{\text{KD}} = T_{\text{KD}}, \; \phi_{\text{TD}} = \phi_{\text{TD}}, \\ & \phi_{\text{GR}} = \phi_{\text{GR,bot}}, \; \phi_{\text{GD}} = \phi_{\text{GD,bot}}, \; F_{\text{TD}} = F_{\text{TD,bot}}, \\ & I_{\text{DSAT}} = I_{\text{DSAT,bot}}, \; V_{\text{bi}} = V_{\text{bi,bot}}, \; V_{\text{bi,min}} = V_{\text{bi,min}}, \; V_{\text{F,min}} = V_{\text{F,min}}, \\ & V_{\text{ch}} = V_{\text{ch}}, \; \textbf{VMAX} = \textbf{VMAX}, \; \textbf{CJOR} = \textbf{CJORBOT}, \\ & \textbf{VBIR} = \textbf{VBIRBOT}, \; \textbf{P} = \textbf{PBOT}, \; \textbf{CSRH} = \textbf{CSRHBOT}, \\ & \textbf{XJUN} = 1, \; \textbf{CTAT} = \textbf{CTATBOT}, \\ & \textbf{MEFFTAT} = \textbf{MEFFTATBOT}, \; \textbf{CBBT} = \textbf{CBBTBOT}, \\ & \textbf{FBBTR} = \textbf{FBBTRBOT}, \; \textbf{STFBBT} = \textbf{STFBBTBOT}, \\ & \textbf{VBR} = \textbf{VBRBOT}, \; \textbf{PBR} = \textbf{PBRBOT} \;) \end{aligned} \tag{4.74}$$

$$
\begin{aligned}
Q'_{\text{j,sti}} \;=\; Q'_{\text{j}}\,(&V_{\text{AK}} = V_{\text{AK}}, \; T_{\text{KR}} = T_{\text{KR}}, \; T_{\text{KD}} = T_{\text{KD}}, \; \phi_{\text{TD}} = \phi_{\text{TD}}, \\
&\phi_{\text{GR}} = \phi_{\text{GR,sti}}, \; \phi_{\text{GD}} = \phi_{\text{GD,sti}}, \; F_{\text{TD}} = F_{\text{TD,sti}}, \\
&I_{\text{DSAT}} = I_{\text{DSAT,sti}}, \; V_{\text{bi}} = V_{\text{bi,sti}}, \; V_{\text{bi,min}} = V_{\text{bi,min}}, \; V_{\text{F,min}} = V_{\text{F,min}}, \\
&V_{\text{ch}} = V_{\text{ch}}, \; \textbf{VMAX} = \textbf{VMAX}, \; \textbf{CJOR} = \textbf{CJORSTI}, \\
&\textbf{VBIR} = \textbf{VBIRSTI}, \; \textbf{P} = \textbf{PSTI}, \; \textbf{CSRH} = \textbf{CSRHSTI}, \\
&\textbf{XJUN} = \textbf{XJUNSTI}, \; \textbf{CTAT} = \textbf{CTATSTI}, \\
&\textbf{MEFFTAT} = \textbf{MEFFTATSTI}, \; \textbf{CBBT} = \textbf{CBBTSTI}, \\
&\textbf{FBBTR} = \textbf{FBBTRSTI}, \; \textbf{STFBBT} = \textbf{STFBBTSTI}, \\
&\textbf{VBR} = \textbf{VBRSTI}, \; \textbf{PBR} = \textbf{PBRSTI} \;)
\end{aligned}
\tag{4.75}
$$

$$
\begin{aligned}
Q'_{\text{j,gat}} \;=\; Q'_{\text{j}}\,(&V_{\text{AK}} = V_{\text{AK}}, \; T_{\text{KR}} = T_{\text{KR}}, \; T_{\text{KD}} = T_{\text{KD}}, \; \phi_{\text{TD}} = \phi_{\text{TD}}, \\
&\phi_{\text{GR}} = \phi_{\text{GR,gat}}, \; \phi_{\text{GD}} = \phi_{\text{GD,gat}}, \; F_{\text{TD}} = F_{\text{TD,gat}}, \\
&I_{\text{DSAT}} = I_{\text{DSAT,gat}}, \; V_{\text{bi}} = V_{\text{bi,gat}}, \; V_{\text{bi,min}} = V_{\text{bi,min}}, \; V_{\text{F,min}} = V_{\text{F,min}}, \\
&V_{\text{ch}} = V_{\text{ch}}, \; \textbf{VMAX} = \textbf{VMAX}, \; \textbf{CJOR} = \textbf{CJORGAT}, \\
&\textbf{VBIR} = \textbf{VBIRGAT}, \; \textbf{P} = \textbf{PGAT}, \; \textbf{CSRH} = \textbf{CSRHGAT}, \\
&\textbf{XJUN} = \textbf{XJUNGAT}, \; \textbf{CTAT} = \textbf{CTATGAT}, \\
&\textbf{MEFFTAT} = \textbf{MEFFTATGAT}, \; \textbf{CBBT} = \textbf{CBBTGAT}, \\
&\textbf{FBBTR} = \textbf{FBBTRGAT}, \; \textbf{STFBBT} = \textbf{STFBBTGAT}, \\
&\textbf{VBR} = \textbf{VBRGAT}, \; \textbf{PBR} = \textbf{PBRGAT} \;)
\end{aligned}
\tag{4.76}
$$

$$
Q_{\text{j}} = \textbf{TYPE} \cdot \textbf{MULT} \cdot \left(\textbf{AB} \cdot Q'_{\text{j,bot}} + \textbf{LS} \cdot Q'_{\text{j,sti}} + \textbf{LG} \cdot Q'_{\text{j,gat}} \right)
\tag{4.77}
$$

4.3.2 Junction current

$$
\begin{aligned}
I'_{\text{j,bot}} \;=\; I'_{\text{j}}\,(&V_{\text{AK}} = V_{\text{AK}}, \; T_{\text{KR}} = T_{\text{KR}}, \; T_{\text{KD}} = T_{\text{KD}}, \; \phi_{\text{TD}} = \phi_{\text{TD}}, \\
&\phi_{\text{GR}} = \phi_{\text{GR,bot}}, \; \phi_{\text{GD}} = \phi_{\text{GD,bot}}, \; F_{\text{TD}} = F_{\text{TD,bot}}, \\
&I_{\text{DSAT}} = I_{\text{DSAT,bot}}, \; V_{\text{bi}} = V_{\text{bi,bot}}, \; V_{\text{bi,min}} = V_{\text{bi,min}}, \; V_{\text{F,min}} = V_{\text{F,min}}, \\
&V_{\text{ch}} = V_{\text{ch}}, \; \textbf{VMAX} = \textbf{VMAX}, \; \textbf{CJOR} = \textbf{CJORBOT}, \\
&\textbf{VBIR} = \textbf{VBIRBOT}, \; \textbf{P} = \textbf{PBOT}, \; \textbf{CSRH} = \textbf{CSRHBOT}, \\
&\textbf{XJUN} = 1, \; \textbf{CTAT} = \textbf{CTATBOT}, \\
&\textbf{MEFFTAT} = \textbf{MEFFTATBOT}, \; \textbf{CBBT} = \textbf{CBBTBOT}, \\
&\textbf{FBBTR} = \textbf{FBBTRBOT}, \; \textbf{STFBBT} = \textbf{STFBBTBOT}, \\
&\textbf{VBR} = \textbf{VBRBOT}, \; \textbf{PBR} = \textbf{PBRBOT} \;)
\end{aligned}
\tag{4.78}
$$

$$
\begin{aligned}
I'_{\text{j,sti}} \;=\; & I'_{\text{j}}\,(V_{\text{AK}} = V_{\text{AK}}, \; T_{\text{KR}} = T_{\text{KR}}, \; T_{\text{KD}} = T_{\text{KD}}, \; \phi_{\text{TD}} = \phi_{\text{TD}}, \\
& \phi_{\text{GR}} = \phi_{\text{GR,sti}}, \; \phi_{\text{GD}} = \phi_{\text{GD,sti}}, \; F_{\text{TD}} = F_{\text{TD,sti}}, \\
& I_{\text{DSAT}} = I_{\text{DSAT,sti}}, \; V_{\text{bi}} = V_{\text{bi,sti}}, \; V_{\text{bi,min}} = V_{\text{bi,min}}, \; V_{\text{F,min}} = V_{\text{F,min}}, \\
& V_{\text{ch}} = V_{\text{ch}}, \; \mathbf{VMAX} = \mathbf{VMAX}, \; \mathbf{CJOR} = \mathbf{CJORSTI}, \\
& \mathbf{VBIR} = \mathbf{VBIRSTI}, \; \mathbf{P} = \mathbf{PSTI}, \; \mathbf{CSRH} = \mathbf{CSRHSTI}, \\
& \mathbf{XJUN} = \mathbf{XJUNSTI}, \; \mathbf{CTAT} = \mathbf{CTATSTI}, \\
& \mathbf{MEFFTAT} = \mathbf{MEFFTATSTI}, \; \mathbf{CBBT} = \mathbf{CBBTSTI}, \\
& \mathbf{FBBTR} = \mathbf{FBBTRSTI}, \; \mathbf{STFBBT} = \mathbf{STFBBTSTI}, \\
& \mathbf{VBR} = \mathbf{VBRSTI}, \; \mathbf{PBR} = \mathbf{PBRSTI} \;)
\end{aligned}
\tag{4.79}
$$

$$
\begin{aligned}
I'_{\text{j,gat}} \;=\; & I'_{\text{j}}\,(V_{\text{AK}} = V_{\text{AK}}, \; T_{\text{KR}} = T_{\text{KR}}, \; T_{\text{KD}} = T_{\text{KD}}, \; \phi_{\text{TD}} = \phi_{\text{TD}}, \\
& \phi_{\text{GR}} = \phi_{\text{GR,gat}}, \; \phi_{\text{GD}} = \phi_{\text{GD,gat}}, \; F_{\text{TD}} = F_{\text{TD,gat}}, \\
& I_{\text{DSAT}} = I_{\text{DSAT,gat}}, \; V_{\text{bi}} = V_{\text{bi,gat}}, \; V_{\text{bi,min}} = V_{\text{bi,min}}, \; V_{\text{F,min}} = V_{\text{F,min}}, \\
& V_{\text{ch}} = V_{\text{ch}}, \; \mathbf{VMAX} = \mathbf{VMAX}, \; \mathbf{CJOR} = \mathbf{CJORGAT}, \\
& \mathbf{VBIR} = \mathbf{VBIRGAT}, \; \mathbf{P} = \mathbf{PGAT}, \; \mathbf{CSRH} = \mathbf{CSRHGAT}, \\
& \mathbf{XJUN} = \mathbf{XJUNGAT}, \; \mathbf{CTAT} = \mathbf{CTATGAT}, \\
& \mathbf{MEFFTAT} = \mathbf{MEFFTATGAT}, \; \mathbf{CBBT} = \mathbf{CBBTGAT}, \\
& \mathbf{FBBTR} = \mathbf{FBBTRGAT}, \; \mathbf{STFBBT} = \mathbf{STFBBTGAT}, \\
& \mathbf{VBR} = \mathbf{VBRGAT}, \; \mathbf{PBR} = \mathbf{PBRGAT} \;)
\end{aligned}
\tag{4.80}
$$

$$
I_{\text{j}} = \mathbf{TYPE} \cdot \mathbf{MULT} \cdot \left(\mathbf{AB} \cdot I'_{\text{j,bot}} + \mathbf{LS} \cdot I'_{\text{j,sti}} + \mathbf{LG} \cdot I'_{\text{j,gat}} \right)
\tag{4.81}
$$

4.3.3 Junction noise

$$
S_{\text{I}} = 2 \cdot q \cdot |I_{\text{j}}|
\tag{4.82}
$$

4.4 JUNCAP Express

The equations in this section are evaluated only if **SWJUNEXP** = 1. Note that only the main model equations are given here. Some details of the implementation, e.g., to avoid numerical issues, are omitted. Please refer to the Verilog-A code of the model [4] for full details.

4.4.1 Calculation of internal parameters

In this section, bias-independent internal parameters for Juncap Express are calculated. All computations in this section are dependent on model/instance parameters and temperature only; they are independent of bias. Therefore, these equations need to be evaluated in the initialization phase only.

Current model initialization

$$
V_1 = -0.4 \cdot \mathbf{VJUNREF}
\tag{4.83}
$$

$$
V_2 = -0.65 \cdot \mathbf{VJUNREF}
\tag{4.84}
$$

$$V_3 = -0.8 \cdot \mathbf{VJUNREF} \tag{4.85}$$

$$V_4 = 0.1 \tag{4.86}$$

$$V_5 = 0.2 \tag{4.87}$$

$$I_n = f_{\mathrm{juncap}}(V_n) \ \text{ for } n = 1 \ldots 5 \tag{4.88}$$

Here, $f_{\mathrm{juncap}}(V)$ is defined as the result of Eq. (4.81) with $V_{\mathrm{AK}} = V$, **MULT** $= 1$, and **TYPE** $= 1$.

$$g(V, I_0, m) = I_0 \cdot [\exp(V \cdot m/\phi_{\mathrm{TD}}) - 1.0] \tag{4.89}$$

Ideal forward current

$$\mathbf{ISATFOR1} = \mathbf{AB} \cdot I_{\mathrm{DSAT,bot}} + \mathbf{LS} \cdot I_{\mathrm{DSAT,sti}} + \mathbf{LG} \cdot I_{\mathrm{DSAT,gat}} \tag{4.90}$$

$$\mathbf{MFOR1} = 1 \tag{4.91}$$

Non-ideal forward current

$$I_{4,\mathrm{cor}} = I_4 - g(V_4, \mathbf{ISATFOR1}, \mathbf{MFOR1}) \tag{4.92}$$

$$I_{5,\mathrm{cor}} = I_5 - g(V_5, \mathbf{ISATFOR1}, \mathbf{MFOR1}) \tag{4.93}$$

$$\alpha_{\mathrm{for}} = I_{4,\mathrm{cor}}/I_{5,\mathrm{cor}} \tag{4.94}$$

$$\mathbf{MFOR2} = \phi_{\mathrm{TD}} \cdot \frac{\ln(\alpha_{\mathrm{for}})}{V_4 - V_5} \tag{4.95}$$

$$\mathbf{ISATFOR2} = \frac{I_{4,\mathrm{cor}}}{\exp(V_4 \cdot \mathbf{MFOR2}/\phi_{\mathrm{TD}}) - 1} \tag{4.96}$$

Reverse current

$$I_{1,\mathrm{cor}} = I_1 - g(V_1, \mathbf{ISATFOR1}, \mathbf{MFOR1}) - g(V_1, \mathbf{ISATFOR2}, \mathbf{MFOR2}) \tag{4.97}$$

$$I_{2,\mathrm{cor}} = I_3 - g(V_2, \mathbf{ISATFOR1}, \mathbf{MFOR1}) - g(V_2, \mathbf{ISATFOR2}, \mathbf{MFOR2}) \tag{4.98}$$

$$I_{3,\mathrm{cor}} = I_3 - g(V_3, \mathbf{ISATFOR1}, \mathbf{MFOR1}) - g(V_3, \mathbf{ISATFOR2}, \mathbf{MFOR2}) \tag{4.99}$$

$$\alpha_{\mathrm{rev}} = I_{1,\mathrm{cor}}/I_{2,\mathrm{cor}} \tag{4.100}$$

$$m_0 = \phi_{\mathrm{TD}} \cdot \frac{\ln \alpha_{\mathrm{rev}}}{V_2 - V_1} \tag{4.101}$$

$$\Delta m = \phi_{\mathrm{TD}} \cdot \frac{(\alpha_{\mathrm{rev}} - 1) \cdot \left(\alpha_{\mathrm{rev}}^{\frac{V_2}{V_2 - V_1}} - 1 \right)}{\alpha_{\mathrm{rev}} \cdot V_1 - V_2 + (V_2 - V_1) \cdot \alpha_{\mathrm{rev}}^{\frac{V_1}{V_1 - V_2}}} \tag{4.102}$$

$$\mathbf{MREV} = m_0 + \Delta m \tag{4.103}$$

$$\mathbf{ISATREV} = \frac{-I_{3,\mathrm{cor}}}{\exp(-V_3 \cdot \mathbf{MREV}/\phi_{\mathrm{TD}}) - 1} \tag{4.104}$$

Charge model initialization

$$C_{\text{jo,bot}} = \textbf{CJORBOT} \cdot \left(\frac{\textbf{VBIRBOT}}{V_{\text{bi,bot}}} \right)^{\textbf{PBOT}} \tag{4.105}$$

$$C_{\text{jo,sti}} = \textbf{CJORSTI} \cdot \left(\frac{\textbf{VBIRSTI}}{V_{\text{bi,sti}}} \right)^{\textbf{PSTI}} \tag{4.106}$$

$$C_{\text{jo,gat}} = \textbf{CJORGAT} \cdot \left(\frac{\textbf{VBIRGAT}}{V_{\text{bi,gat}}} \right)^{\textbf{PGAT}} \tag{4.107}$$

$$Z_{\text{bot}} = \textbf{AB} \cdot C_{\text{jo,bot}} \tag{4.108}$$

$$Z_{\text{sti}} = \textbf{LS} \cdot C_{\text{jo,sti}} \tag{4.109}$$

$$Z_{\text{gat}} = \textbf{LG} \cdot C_{\text{jo,gat}} \tag{4.110}$$

$$Z_{\text{tot}} = Z_{\text{bot}} + Z_{\text{sti}} + Z_{\text{gat}} \tag{4.111}$$

4.4.2 JUNCAP Express model equations

The equations given below have to be evaluated at each bias step. The very idea behind the JUNCAP Express model is that these equations have been kept very simple, at the expense of a much more complicated model initialization.

Currents

$$I_{\text{for1}} = g(V_{\text{AK}}, \textbf{ISATFOR1}, \textbf{MFOR1}) \tag{4.112}$$

$$I_{\text{for2}} = g(V_{\text{AK}}, \textbf{ISATFOR2}, \textbf{MFOR2}) \tag{4.113}$$

$$I_{\text{rev}} = -g(-V_{\text{AK}}, \textbf{ISATREV}, \textbf{MREV}) \tag{4.114}$$

$$I_{\text{j}} = \textbf{TYPE} \cdot \textbf{MULT} \cdot (I_{\text{for1}} + I_{\text{for2}} + I_{\text{rev}}) \tag{4.115}$$

Charge model

$$V_{\text{j}} = \text{hyp}_5(V_{\text{AK}}; V_{\text{F,min}}, V_{\text{ch}}) \tag{4.116}$$

$$Q'_{\text{j,bot}} = \begin{cases} \left\{ \dfrac{C_{\text{jo,bot}} \cdot V_{\text{bi,bot}}}{1 - \textbf{PBOT}} \cdot \left[1 - \left(1 - \dfrac{V_{\text{j}}}{V_{\text{bi,bot}}} \right)^{1-\textbf{PBOT}} \right] \right. \\ \qquad\qquad\qquad \left. + a \cdot C_{\text{jo,bot}} \cdot (V_{\text{AK}} - V_{\text{j}}) \right\} & \text{if } Z_{\text{bot}} > \textbf{FJUNQ} \cdot Z_{\text{tot}} \\ \\ 0 & \text{otherwise} \end{cases} \tag{4.117}$$

$$Q'_{\text{j,sti}} = \begin{cases} \left\{ \dfrac{C_{\text{jo,sti}} \cdot V_{\text{bi,sti}}}{1 - \textbf{PSTI}} \cdot \left[1 - \left(1 - \dfrac{V_{\text{j}}}{V_{\text{bi,sti}}} \right)^{1-\textbf{PSTI}} \right] \right. \\ \qquad\qquad\qquad \left. + a \cdot C_{\text{jo,sti}} \cdot (V_{\text{AK}} - V_{\text{j}}) \right\} & \text{if } Z_{\text{sti}} > \textbf{FJUNQ} \cdot Z_{\text{tot}} \\ \\ 0 & \text{otherwise} \end{cases} \tag{4.118}$$

$$
Q'_{j,gat} =
\begin{cases}
\left\{ \dfrac{C_{jo,gat} \cdot V_{bi,gat}}{1 - \mathbf{PGAT}} \cdot \left[1 - \left(1 - \dfrac{V_j}{V_{bi,gat}} \right)^{1-\mathbf{PGAT}} \right] \right. \\
\qquad\qquad\qquad \left. + a \cdot C_{jo,gat} \cdot (V_{AK} - V_j) \right\} & \text{if } Z_{gat} > \mathbf{FJUNQ} \cdot Z_{tot} \\[3mm]
0 & \text{otherwise}
\end{cases}
\tag{4.119}
$$

$$
Q_j = \mathbf{TYPE} \cdot \mathbf{MULT} \cdot \left(\mathbf{AB} \cdot Q'_{j,bot} + \mathbf{LS} \cdot Q'_{j,sti} + \mathbf{LG} \cdot Q'_{j,gat} \right)
\tag{4.120}
$$

Noise

$$
S_I = 2 \cdot q \cdot |I_j|
\tag{4.121}
$$

Section 5

DC operating point output

The DC operating point output facility gives information on the state of a device at its operating point. Note that—conform the PSP model operating point output—the information is always given as if **TYPE** = 1. E.g., in forward bias both **vak** and **ij** are positive.

No.	Name	Unit	Value	Description
0	**vak**	V	V_{AK}	voltage between anode and cathode
1	**cj**	F	**cjbot+cjsti+ cjgat**	total junction capacitance
2	**cjbot**	F	$\mathbf{MULT} \cdot \mathbf{AB} \cdot \partial Q'_{\mathrm{j,bot}}/\partial V_{\mathrm{AK}}$	bottom component of the junction capacitance
3	**cjsti**	F	$\mathbf{MULT} \cdot \mathbf{LS} \cdot \partial Q'_{\mathrm{j,sti}}/\partial V_{\mathrm{AK}}$	STI-edge component of the junction capacitance
4	**cjgat**	F	$\mathbf{MULT} \cdot \mathbf{LG} \cdot \partial Q'_{\mathrm{j,gat}}/\partial V_{\mathrm{AK}}$	gate-edge component of the junction capacitance
5	**ij**	A	**ijbot+ijsti+ ijgat**	total junction current
6	**ijbot**	A	$\mathbf{MULT} \cdot \mathbf{AB} \cdot I'_{\mathrm{j,bot}}$	bottom component of the junction current
7	**ijsti**	A	$\mathbf{MULT} \cdot \mathbf{LS} \cdot I'_{\mathrm{j,sti}}$	STI-edge component of the junction current
8	**ijgat**	A	$\mathbf{MULT} \cdot \mathbf{LG} \cdot I'_{\mathrm{j,gat}}$	gate-edge component of the junction current
9	**si**	A^2/Hz	S_{I}	total junction current noise spectral density

Note: If **SWJUNEXP** = 1, only a total junction current is computed, not the three separate components. Therefore, **ijbot**, **ijsti**, and **ijgat** are all set to 0 in that case and **ij** is the total junction current.

Section 6

Parameter extraction

6.1 Test structures

For extraction of JUNCAP2 parameters, one needs three different test structures, depicted schematically in Figure 6.1. The first structure is a simple, square diode, which has a large bottom component, a relatively small STI-edge component, and no gate-edge component. The second structure is a finger diode, which has a much larger STI-edge component, and no gate-edge component. The third structure is a Miller diode, which is nothing else than a multi-fingered MOSFET with source and drains tied together. It has a relatively small STI-edge component, and a significant gate-edge component. Besides the three test structures described here, which are needed for parameter extraction, one can optionally use additional geometries for verification purposes. The test structures should be sufficiently large so that currents and capacitances are easily measurable.
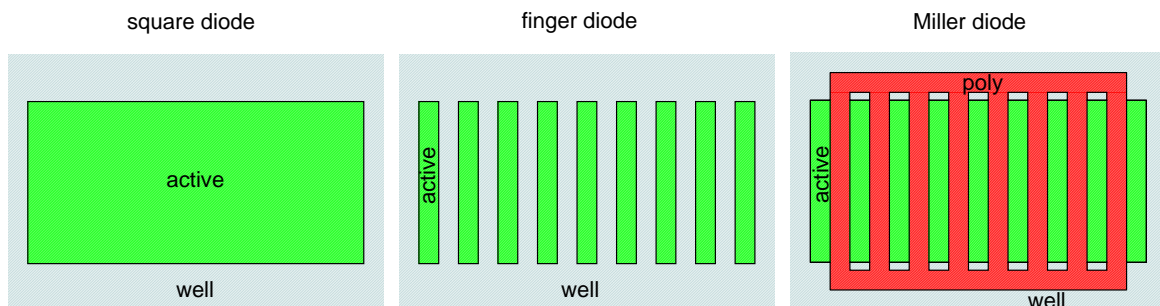
Figure 6.1: Schematic representation of three test structures needed for parameter extraction.

6.2 Measurements

For extraction of JUNCAP2 parameters, one needs both CV and IV measurements. The IV data should be taken over a large range of temperatures, ranging from -40 °C to at least 125 °C. If available, even higher temperatures can be very helpful in the extraction because the junction current tends more and more to ideal behavior at higher temperatures.

Because the temperature dependence of capacitance is fairly low, it is possible (but not recommended) to restrict oneself to room-temperature CV measurements only. For optimal accuracy of the capacitance model however, measurements at different temperature are needed. Therefore it is recommended to take the CV data at the same temperatures as the IV data.

All IV measurements should be done from reverse bias ($-V_{\text{supply}}$) up to small forward bias (e.g. 0.5 V). If avalanche breakdown parameters need to be extracted, one needs to do additional measurements with a reverse bias much larger than the supply voltage. Because the JUNCAP2 model has no parameters to model temperature dependence of the breakdown, it suffices to do this breakdown characterization at room temperature. In the IV measurements, it is recommended to apply a current compliance (e.g. 10 mA) to avoid damaging the test structures when they are biased in the forward regime or in the avalanche breakdown regime.

The CV measurements should be done from reverse bias ($-V_{\text{supply}}$) up to zero bias. CV measurements in the forward mode of operation rapidly become unreliable because the phase angle starts to deviate from $90°$ quickly. When the junction capacitance is measured on a Miller diode, the gate should be grounded.

6.3 Extraction of bottom, STI-edge, and gate-edge components

All measurements are carried out on three test structures. The measurements on these three structures are used to extract the three components (bottom, STI-edge, and gate-edge components) of either current or capacitance. For the capacitance, the extraction procedure will be outlined below.

For the capacitance of the square diode and finger diode, both having zero gate edge, we can write:

$$C_{\text{j,square}} = \mathbf{AB}_{\text{square}} \cdot C'_{\text{j,bot}} + \mathbf{LS}_{\text{square}} \cdot C'_{\text{j,sti}} \tag{6.1}$$

$$C_{\text{j,finger}} = \mathbf{AB}_{\text{finger}} \cdot C'_{\text{j,bot}} + \mathbf{LS}_{\text{finger}} \cdot C'_{\text{j,sti}} \tag{6.2}$$

For the Miller diode, we write:

$$C_{\text{j,Miller}} = \mathbf{AB}_{\text{Miller}} \cdot C'_{\text{j,bot}} + \mathbf{LS}_{\text{Miller}} \cdot C'_{\text{j,sti}} + \mathbf{LG}_{\text{Miller}} \cdot C'_{\text{j,gat}} \tag{6.3}$$

From Eqs. (6.1) and (6.2) we straightforwardly solve the two unknowns $C'_{\text{j,bot}}$ and $C'_{\text{j,sti}}$:

$$C'_{\text{j,bot}} = \frac{\mathbf{LS}_{\text{finger}} \cdot C_{\text{j,square}} - \mathbf{LS}_{\text{square}} \cdot C_{\text{j,finger}}}{\mathbf{LS}_{\text{finger}} \cdot \mathbf{AB}_{\text{square}} - \mathbf{LS}_{\text{square}} \cdot \mathbf{AB}_{\text{finger}}} \tag{6.4}$$

$$C'_{\text{j,sti}} = \frac{\mathbf{AB}_{\text{square}} \cdot C_{\text{j,finger}} - \mathbf{AB}_{\text{finger}} \cdot C_{\text{j,square}}}{\mathbf{LS}_{\text{finger}} \cdot \mathbf{AB}_{\text{square}} - \mathbf{LS}_{\text{square}} \cdot \mathbf{AB}_{\text{finger}}} \tag{6.5}$$

And now we can derive the final unknown quantity $C'_{\text{j,gat}}$ from Eq. (6.3):

$$C'_{\text{j,gat}} = \frac{C_{\text{j,Miller}} - \mathbf{AB}_{\text{Miller}} \cdot C'_{\text{j,bot}} - \mathbf{LS}_{\text{Miller}} \cdot C'_{\text{j,sti}}}{\mathbf{LG}_{\text{Miller}}} \tag{6.6}$$

The procedure as outlined above is also applied to the junction currents, resulting in the current components $I'_{\text{j,bot}}$, $I'_{\text{j,sti}}$, and $I'_{\text{j,gat}}$.

6.4 Extraction of CV parameters

Having extracted the current and capacitance components as explained in Section 6.3, we are ready for the actual parameter extraction.

First, one has to set some general parameters:

- **LEVEL** is equal to 200 for the first release of the JUNCAP2 model. Possible successors will be 201, 202, etc.

- **TYPE** should be set properly to select either $n - p$ or $p - n$ junction.

- **DTA** should be set to zero

- **IMAX** should be set to a value which is large enough (e.g. larger than the highest forward current measured) so that it does not affect the extraction procedure.

Before IV parameter extraction is started, it is mandatory to perform the CV extraction first, because the CV parameters are used throughout the IV model. In other words, changing CV parameters *after* IV parameter extraction will change not only the CV curves, but also the IV curves.

The CV parameter extraction is basically the same for the three components. Therefore we will restrict the description to the bottom component. The **PHIGBOT** has to be initialized to a reasonable value, e.g. 1.16 V. (It will be fitted later on to the forward IV curves, but this usually has a negligible effect on the CV curves). If needed, one From the CV curves, one extracts three parameters per component:

- **CJORBOT**, i.e. the zero-bias capacitance per unit of area at the reference temperature. Its initial value is directly taken from the $C'_{j,bot}$ curves. One should select the $C'_{j,bot}$ curve measured at the temperature closest to the reference temperature, and use the zero-bias $C'_{j,bot}$ value of that curves as starting value for **CJORBOT**.

- **PBOT**, i.e. the grading coefficient. As starting value one can take **PBOT** $= 0.5$.

- **VBIRBOT**, i.e. the junction built-in voltage at the reference temperature As starting value one can take **VBIRBOT** $= 1$.

Using the starting values specified above, one can perform a least-square fit of these three parameters to the measured CV curves. Typical values for the grading coefficient are between 0.3 and 0.6. Typical values for the built-in voltage are between 0.5 V and 1.2 V (from physics, we know that this quantity may exceed the band gap voltage only slightly).

6.5 Extraction of IV parameters

Ideal-current parameters

The IV parameter extraction starts with the extraction of the ideal-current parameters, which are **IDSATRBOT** and **PHIGBOT** (we restrict ourselves again to the bottom component). The parameter **IDSATRBOT** has effect on the ideal current only. The parameter **PHIGBOT** is used throughout the model. The ideal-current parameters are extracted on those parts of the forward IV curves which shown nearly ideal behavior. These parts are selected using the ideality factor n_{bot} which can be determined from the forward IV measurements as follows:

$$n_{bot} = \left(\phi_{TD} \cdot \frac{\partial \ln I'_{j,bot}}{\partial V_{AK}} \right)^{-1} \tag{6.7}$$

For the fitting of the ideal-current parameters we select those measurement points, for which the ideality factor is reasonably close to 1. For instance, the criterion $n_{bot} > 0.9$ works well for this purpose. Because the parameter **PHIGBOT** has already been initialized to 1.16, we only need to worry about a starting value for **IDSATRBOT**. This starting value can be found by setting **IDSATRBOT** to 1, and calculate the average ratio of measured and modelled current in the region selected by the ideality-factor method. (Note: this can only be done successfully when **IMAX** is temporarily set to a huge value.) After this initialization, modelled and measured curves should be reasonably close and one can further optimize the parameters **IDSATRBOT** and **PHIGBOT** using a least-square fit of the model to the measurement points selected by the ideality-factor method.

Please note once more that this ideality factor is only a quantity directly derived from measurements. It is not a model parameter as in many other junction models.

Identification of leakage mechanisms

The next step is the extraction of the remaining leakage current parameters. First, one needs to get an idea which effects need to be included. Sometimes, only Shockley-Read-Hall and trap-assisted tunneling are relevant, sometimes only band-to-band-tunneling, sometimes both. To this purpose one may investigate the temperature dependence by inspection of the activation energy of the leakage currents, which is calculated (in eV) as follows:

$$E_{\text{act}} = \frac{\partial \ln \left(I'_{\text{j,bot}} \right)}{\partial \phi_{\text{TD}}^{-1}} \tag{6.8}$$

An activation energy close to the bandgap (1.16 eV) is an indication that the current is ideal. An activation energy around half the bandgap is an indication that the current is dominated by Shockley-Read-Hall and trap-assisted tunneling. An activation energy well below half the bandgap is an indication that the current is dominated by band-to-band-tunneling.

Not only the temperature dependence (as expressed in terms of activation energy), but also the bias dependence is indicative for the mechanisms behind the observed reverse junction current. The ideal current has no bias dependence (for reverse biases in excess of a few times the thermal voltage). Shockley-Read-Hall and trap-assisted tunneling have much more significant bias dependence. For Shockley-Read-Hall, the bias dependence goes approximately as the square root of the voltage. For trap-assisted tunneling, due to the field-enhancement, the bias dependence is larger. The largest bias dependence however is seen in case of band-to-band tunneling.

In conclusion, inspection of both temperature and bias dependence of the reverse current helps to identify the relevant leakage mechanism(s) in the junction component under investigation.

Extraction Shockley-Read-Hall and trap-assisted tunneling parameters

The fitting of Shockley-Read-Hall and trap-assisted tunneling parameters goes as follows. First, one needs to initialize the relevant parameters:

1. **MEFFTATBOT** should be initialized to 0.25. It will be fitted to the data later and affects the bias dependence of the trap-assisted tunneling current.

2. **XJUNSTI** or **XJUNGAT** should be initialized to a physically reasonable value (between 10 and 100 nm for modern CMOS). There is obviously no **XJUN** for the bottom component.

3. **CTATBOT** = **CSRHBOT**. A good starting value is found as follows. First, set **CTATBOT** and **CSRHBOT** equal to 1 and calculate the junction current. The required starting value is now found by averaging the ratio of measured and modelled currents for those reverse-bias points which are selected using the activation-energy method. A suitable criterion to select those bias points is $0.3\,\text{V} < \text{E}_{\text{act}} < 0.7\,\text{V}$.

After this initialization the parameters **CTATBOT** = **CSRHBOT**, **MEFFTATBOT** are optimized by a least-square fit of the parameters to the measured data. For the STI-edge and gate-edge components also the parameters **XJUNSTI** resp. **XJUNGAT** may be optimized. Usually a good fit can be achieved while retaining the identity **CTATBOT** = **CSRHBOT**. The parameter **MEFFTATBOT** is sometimes seen to deviate from the value of 0.25 expected theoretically. One should be able to retain a physically reasonable value for the **XJUN** parameter, in case of STI-edge and gate-edge components, although it is difficult to retain the expected identity **XJUNSTI** = **XJUNGAT**.

Extraction band-to-band tunneling parameters

If band-to-band tunneling is of importance, one needs to initialize the relevant parameters:

1. **FBBTRBOT** should be initialized to 1×10^9 V/m. It will be fitted to the data later, and affects the bias dependence of the band-to-band tunneling current.

© NXP Semiconductors 2009

2. **STFBBTBOT** should be initialized to -1×10^{-3}. It will be fitted to the data later, and affects the temperature dependence dependence of the band-to-band tunneling current.

3. **CBBTBOT**. A good starting value is found as follows. First, set **CBBTBOT** to 1 and calculate the junction current. The required starting value is now found by averaging the ratio of measured and modelled currents for those reverse-bias points which are selected using the activation-energy method. A suitable criterion to select those bias points is $E_{\text{act}} < 0.2$ V.

After this initialization the parameters are optimized by a least-square fit of the parameters to the measured data.

Extraction avalanche breakdown parameters

The breakdown voltage **VBRBOT** is easily found by inspection of the breakdown measurement curves: at $V = -\textbf{VBRBOT}$ a sharp increase in the current is observed. The parameter **PBRBOT** can be used to tune the onset to breakdown. Again, a least-squares curve fit can be used to get a good fit. It is important to check that the Shockley-Read-Hall, trap-assisted-tunneling, and band-to-band tunneling model extrapolate well to the regime of avalanche breakdown. Sometimes, one needs to tune the corresponding parameters slightly to accomplish this.

6.6 General extraction scheme

Here we list a general extraction scheme which should work for most junctions. But please be aware that parameter extraction can never be a "push-button" exercise. The parameter extraction may have to be adapted to specific cases.

1. fit CV parameters;

2. fit ideal current parameters;

3. fit Shockley-Read-Hall and trap-assisted tunneling parameters;

4. fit band-to-band tunneling parameters;

5. fit full IV curves, except avalanche curve, once more with all relevant parameters;

6. fit avalanche breakdown parameters;

7. re-fit CV parameters (because bandgap voltage may have changed);

8. re-fit full IV curves, except avalanche curve, once more with all relevant parameters, except the bandgap voltage: this is needed because the capacitance may have changed, which affects the current;

9. calculate all model curves once more.

6.7 Simulation time considerations

First, simulation time considerations for the full JUNCAP2 model will be discussed. In the last section, the JUNCAP2 Express model—which was especially designed to greatly reduce simulation time—is treated.

6.7.1 Full JUNCAP2 model

MOSFET junction models are computationally expensive by their very nature: every MOSFET has at least *two* junctions (source, drain); each junction has *three* components (bottom, STI-edge, gate-edge); each current component, in turn, can have as much as *five* different conduction mechanisms (ideal, SRH, TAT, BBT, avalanche). Moreover, the physics of junctions is ruled by computationally expensive functions such as powers and exponents.

JUNCAP2 has been constructed in such a way that calculations are skipped when junction components and/or current mechanisms are set to zero. For instance, when BBT is not needed in the bottom component of a junction, one can set **CBBTBOT** to zero, and the corresponding calculation is entirely skipped.

Considerable amount of simulation time can be saved when negligible current contributions are completely switched off in a parameter set that is being extracted. Thus, in the above-mentioned example, instead of leaving **CBBTBOT** at a small, negligible non-zero value, one should set **CBBTBOT** to exactly zero in order to avoid unnecessary function evaluations when the model is used by circuit designers.

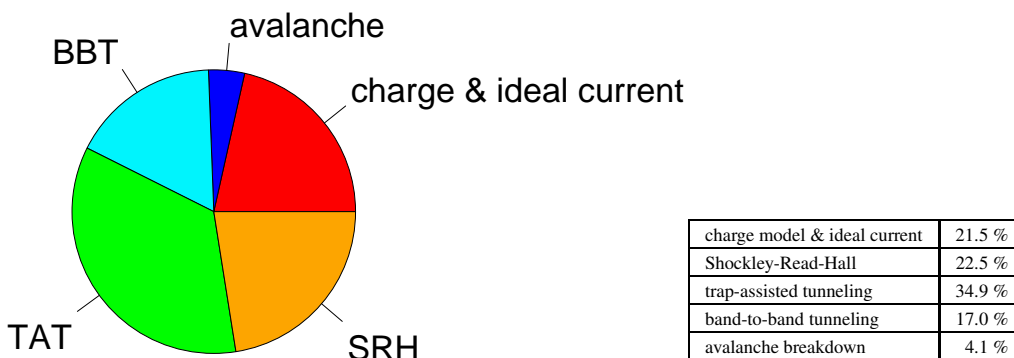| charge model & ideal current | 21.5 % |
Shockley-Read-Hall	22.5 %
trap-assisted tunneling	34.9 %
band-to-band tunneling	17.0 %
avalanche breakdown	4.1 %

Figure 6.2: Typical distribution of simulation times over the various parts of the model. Results were obtained for JUNCAP2, level 200.1 using the Spectre circuit simulator and SiMKit 2.3.2 on a LINUX platform. Note that switching off the ideal current does not lead to significant CPU time savings.

In Fig. 6.2 a typical result for the contribution of the various parts of the JUNCAP2 model to the total JUNCAP2 simulation time is depicted. (Note that the results may be different for different simulators or operating systems). It is observed that SRH, TAT, and BBT are very significant contributors to the overall JUNCAP2 simulation time. Therefore it is useful to check for each junction component (bottom, STI-edge, gate edge) whether it is possible to switch off one or more of these physical effects without affecting the model accuracy too much. It should be noted that switching off the SRH effect only decreases the simulation time when the corresponding TAT parameter is also switched off. The reason for this is that the TAT equations make use of quantities calculated in the SRH equations. Therefore the SRH part of the equations is also calculated in the situation when SRH is switched off and TAT is switched on. Switching off TAT, on the other hand, always decreases the simulation time, irrespective of the value of the corresponding SRH parameter.

For a typical case, the JUNCAP2 features that are needed are given in Table 6.1. Typically, the number of current components needed is only half of the totally available current components. Often, the BBT component of the gate-edge component dominates the reverse leakage, in which case additional CPU time savings can be achieved by switching off SRH and TAT for this junction component.

For completeness' sake, we recapitulate here once more how to switch off the different current components (see also Table 6.2): for the bottom component, the ideal current, SRH current, TAT current, and BBT current are switched off by setting the parameters **IDSATRBOT**, **CSRHBOT**, **CTATBOT**, **CBBTBOT** to zero, respectively. The breakdown model is skipped by setting **VBRBOT** to a value larger than 1000. The procedure for STI-edge and gate-edge currents is, *mutatis mutandis*, the same. Note that it is *not* possible to switch off junction capacitances, because in JUNCAP2 the junction capacitances are internally used to calculate electric fields, and thus influence the junction currents.

Finally, when a geometrical component is not needed, the corresponding instance parameter (**AB**, **LS**, or **LG**) can be set to zero and the calculation for that component is completely skipped. An example is the well diode

of a p-channel MOSFET which has no gate-edge contribution (**LG** $= 0$).

JUNCAP2 feature	geometrical component		
	gate-edge	STI-edge	bottom
capacitance	•	•	•
ideal current	•		•
SRH current	•		•
TAT current	•		•
BBT current	•		
breakdown current	•		

Table 6.1: Guideline for which JUNCAP2 features to take into account in JUNCAP2 parameter extraction.

JUNCAP2 feature	parameter value needed to switch off feature		
	bottom	STI-edge	gate-edge
ideal current	**IDSATRBOT** $= 0$	**IDSATRSTI** $= 0$	**IDSATRGAT** $= 0$
SRH current	**CSRHBOT** $= 0$	**CSRHSTI** $= 0$	**CSRHGAT** $= 0$
TAT current	**CTATBOT** $= 0$	**CTATSTI** $= 0$	**CTATGAT** $= 0$
BBT current	**CBBTBOT** $= 0$	**CBBTSTI** $= 0$	**CBBTGAT** $= 0$
breakdown current	**VBRBOT** > 1000	**VBRSTI** > 1000	**VBRGAT** > 1000

Table 6.2: How to switch off JUNCAP2 features.

6.7.2 JUNCAP2 Express

From JUNCAP2 version 200.3 onwards, the JUNCAP2 model has an express-option, which can be invoked by setting **SWJUNEXP** $= 1$.

Currents

In the Express version of the JUNCAP2 model, the full set of IV-equations in the bias dependent section of the model is replaced by a greatly simplified set of equations (just three exponentials). This leads to a greatly reduced simulation time of the JUNCAP2 model. The initialization of the Express model is much more complex, but as this is carried out only once in an entire simulation, its contribution to the total simulation time is negligible.

Note that—contrary to the full JUNCAP2 model—in the Express version the simulation time is independent of the number of current-components which are switched on/off. Therefore, the results in Fig. 6.2 do *not* apply to the Express model.

Charges

The new parameter **FJUNQ** can be used to reduce the simulation time of the charge-model. In many cases, one or two of the three (bottom, sti-edge, gate-edge) components to the total junction capacitance is negligible. In the Express model, any capacitance component which contributes less then (approximately) a fraction **FJUNQ** to the total capacitance is ignored. This allows the user to save up to 2/3 of the computation time associated with the charge model, with a limited (adjustable) loss of accuracy. When the Express model is invoked, the charge model actually dominates the total evaluation time of the model. Therefore, this feature leads indeed to yet another significant reduction of the total evaluation time.

If necessary, setting **FJUNQ** $= 0$ ensures that all components are taken into account under all circumstances and the full charge model is always evaluated.

References

[1] JUNCAP1 model code and documentation, available for download at `http://www.nxp.com/models/`

[2] G.A.M. Hurkx, D.B.M. Klaassen, and M.P.G. Knuvers, *A new recombination model for device simulation including tunneling*, IEEE Trans. El. Dev., Vol. 39, No. 2, pp. 331–338, February 1992.

[3] W. Jin, C.H. Chan, S.K.H. Fung, and P.K. Ko, *Shot-noise-induced excess low-frequency noise in floating-body partially depleted SOI MOSFET's*, IEEE Trans. El. Dev., Vol. 46, No. 6, pp. 1180–1185, June 1999.

[4] JUNCAP2 model code and documentation, available for download at `http://www.nxp.com/models/`

[5] "MOS Model, level 903", available for download at `http://www.nxp.com/models/`

Appendix A

Auxiliary equations

In this appendix, the hyp-functions that are used in the JUNCAP model equations are defined. These functions have been adopted from MOS Model 9, and their naming is consistent with the MOS Model 9 description [5]. The functions hyp_1, hyp_2, and hyp_5 are given by Eqs. (A.1), (A.2), and (A.3), respectively, and illustrated in Figs. A.1, A.2, and A.3, respectively.

$$\mathrm{hyp}_1(x;\epsilon) = \frac{1}{2} \cdot \left(x + \sqrt{x^2 + 4 \cdot \epsilon^2} \right) \tag{A.1}$$

$$\mathrm{hyp}_2(x;x_0,\epsilon) = x - \mathrm{hyp}_1(x - x_0; \epsilon) \tag{A.2}$$

$$\mathrm{hyp}_5(x;x_0,\epsilon) = x_0 - \mathrm{hyp}_1(x_0 - x - \frac{\epsilon^2}{x_0}; \epsilon) \tag{A.3}$$
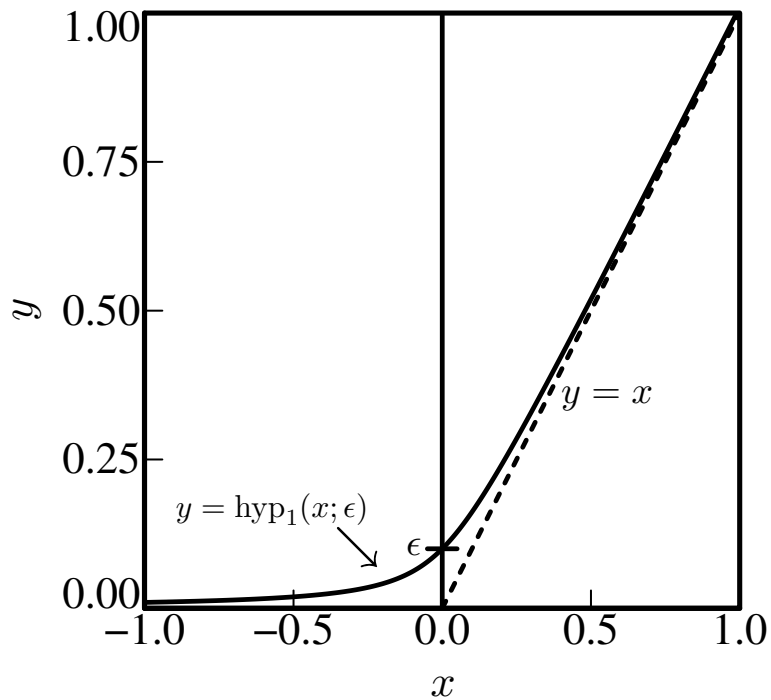

Figure A.1: Solid line: the function $y = \mathrm{hyp}_1(x;\epsilon)$. Dashed line: the $y = x$ asymptote.
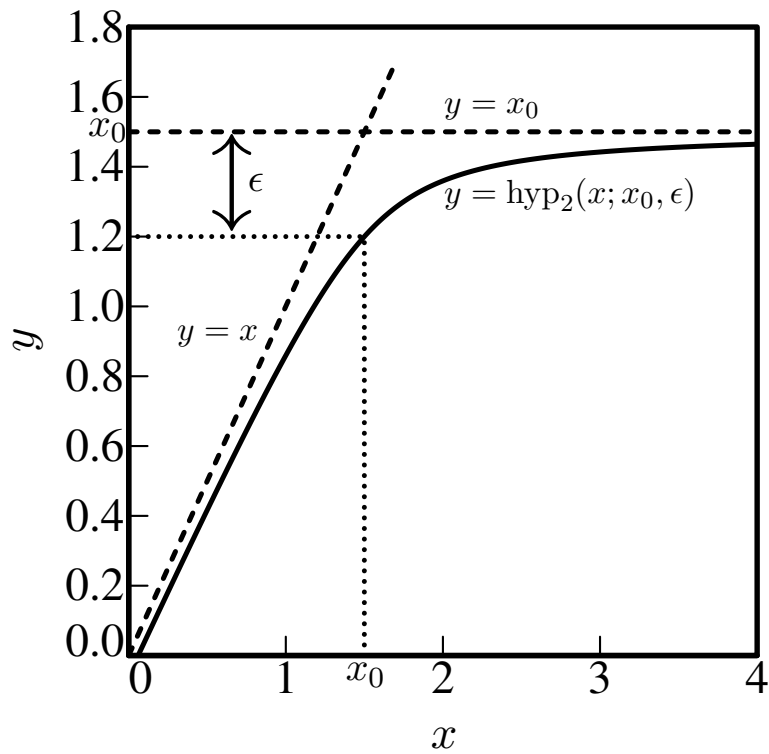
Figure A.2: Solid line: the function $y = \mathrm{hyp}_2(x; x_0, \epsilon)$. Dashed lines: the $y = x$ and $y = x_0$ asymptotes.
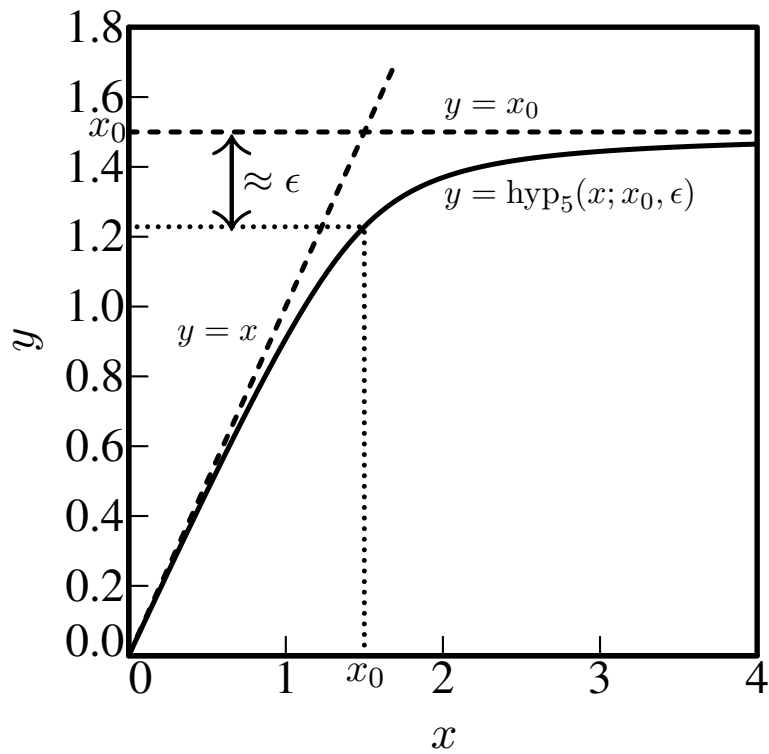

Figure A.3: Solid line: the function $y = \mathrm{hyp}_5(x; x_0, \epsilon)$. Dashed lines: the $y = x$ and $y = x_0$ asymptotes.